Investigation of postoxidation thermal treatments of Si/SiO_2 interface in relationship to the kinetics of amorphous Si suboxide decomposition

B. J. Hinds,[a] F. Wang, D. M. Wolfe, C. L. Hinkle, and G. Lucovsky
Department of Physics, North Carolina State University, Raleigh, North Carolina 27695-8202

(Received 21 January 1998; accepted 21 May 1998)

Interfacial Si suboxides (SiO_x, $x<2$) are detrimental to transistor performance and are typically minimized during postoxidation anneals. To study the kinetics of SiO_x decomposition, thick films (~2000 Å) of amorphous Si:O:H alloys ($0.7<x<1.4$) were deposited by remote plasma enhanced chemical vapor deposition and subjected to rapid thermal anneals. Films were characterized by Fourier transform infrared spectroscopy, Raman spectroscopy, ellipsometry, photoluminescence (PL), and transmission electron microscopy. At temperatures >500 °C initially there is a rapid segregation into amorphous Si (a-Si) surrounded by a SiO_2 shell which acts as a diffusion barrier decelerating the reaction. Phenomenological modeling of kinetics with a one-dimensional Avrami–Erofe've treatment gives an upper limit for a-Si lateral growth rates of 1.2 Å/s at 900 °C with an activation energy of 120 kJ/mol. PL, Raman, transmission electron microscopy and ellipsometry confirm this segregation model in the amorphous state. Due to the rapid initial decomposition and relatively large diffusion coefficients, a simple kinetic hindrance explanation for the 4–8 Å of SiO_x at the SiO_2/Si interface is unlikely. © *1998 American Vacuum Society*. [S0734-211X(98)09104-5]

I. INTRODUCTION

Due to its dominating effects in metal–oxide–semiconductor field-effect transistor (MOSFET) performance, the Si/SiO_2 interface is the subject of extensive studies. This interface is well known to be stoichiometric SiO_2 within 4–6 Å of the interface where suboxides, SiO_x ($x<2$) are seen.[1,2] The amount and nature of the suboxides at the interface is highly dependent on surface preparation, annealing temperatures, and growth temperatures.[1] Solid $SiO_{1.0}$ is thermodynamically unstable below 1173 °C,[3] and decomposes as in Eq. (1). Typically, suboxides in a MOSFET are minimized during a postoxidation anneal. However the quantification of suboxide by x-ray photoelectron spectroscopy (XPS) after this process is extremely difficult due to attenuation of signal from buried interface. If ultrathin oxides are used, the volatilization of SiO gas during anneals becomes significant. It is thus of interest to study the kinetics of Si suboxide disproportionation in bulk samples which can be related to the interface:

$$SiO_x \rightarrow \frac{x}{2}\,SiO_2 + \left(1-\frac{x}{2}\right)Si. \tag{1}$$

Solid $SiO_{1.0}$ grown from evaporation is highly pyrophoric and difficult to study, while H termination stabilized Si suboxides can be synthesized by chemical vapor deposition of semi-insulating polysilicon (SIPOS) or by remote plasma enhanced chemical vapor deposition (RPECVD). Early reports show that SIPOS films decompose into Si_{nc} and amorphous SiO_2 matrix[4] as expected in Eq. (1) and have been studied further,[5–8] however none of these studies closely examined the temperature region, where ultrathin MOSFET gate dielectric growth is important (700–900 °C). There is one report of SiO_x decomposition kinetics in SIPOS films which is derived from measurement of Si nanocrystal size.[9] However, that study measured a crystallization process and is insensitive to reactions in the amorphous state. RPECVD derived films of SiO_x have been shown to similarly form Si_{nc} in SiO_2 matrix after anneals of 900 °C.[10] Therefore it is of interest to study the SiO_x decomposition kinetics with a method insensitive to crystallization processes at temperatures less than 1000 °C.

II. EXPERIMENT

A RPECVD reactor previously described[11] was employed to grow thin films SiO_x ($0.7<x<1.4$). 100 sccm He with 0.05 to 0.2% O_2 was passed through the rf plasma coil tube with 33 W power at 13.56 MHz. 10 sccm of 10% SiH_4/He was introduced through a showerhead ring downstream from the plasma source. Total pressure was maintained at 300 mTorr as well as a substrate temperature of 160 °C. Film thicknesses were typically 2000 Å (16 Å/min). For H_2 plasma treatments, a plasma was generated with 100 sccm of He passing through the plasma coil (50 W power) and 30 sccm of H_2 was introduced downstream with a total pressure of 100 mTorr. The sample was heated to 300 °C and treated for 2 h.

The suboxide films were then annealed *ex situ* in an AG Associates rapid thermal annealing (RTA) furnace under 1 atm of Ar for times of 5 s–3 min (ramp rate 60 °C/s). Fourier transform infrared (FTIR) measurements were performed with a Nicolet 750 spectrometer in transmission mode with a resolution of 4 cm^{-1}. Spectra were subtracted from a reference sample cut from the same Si(100) single side chemically roughened wafer to prevent internal reflection errors. To assure low experimental scatter (from film to film variation), films for each series were annealed sequentially, unless stated otherwise. Photoluminescence (PL) data measurements utilized a capacitance–voltage integrated (CVI) model

[a]Electronic mail: bruce_hinds@ncsu.edu

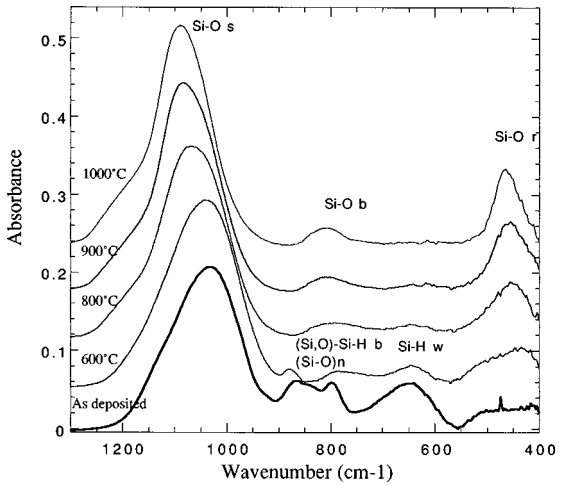

FIG. 1. FTIR absorbance for $SiO_{1.0}$ film after various sequential anneals for 6 min at each temperature, showing blue shift in ν_{Si-O} as well as loss of Si–H bonds. Spectra are offset by 0.06 abs units for clarity. Integrated area under Si–O stretch remains constant for all anneals.

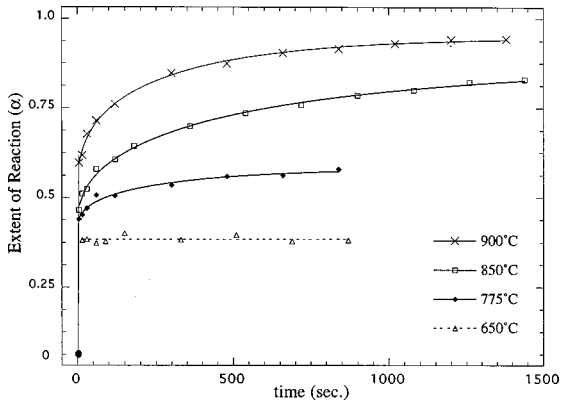

FIG. 2. Extent of reaction (α) for initial $SiO_{0.93}$ thin film as a function of time at various annealing temperatures, showing kinetic metastability of Si suboxides. Curve shown is guide to eye. For each temperature the same film is annealed sequentially to reduce experimental scatter.

DK480 single monochromator with a R928 photomultiplier. A Spectra Physics Ar^+ laser at 488 nm (2.54 eV) provided 100 mW incident excitation energy. Spectral response was calibrated to a standard tungsten–halogen lamp. Conductivity measurements were made at 100 V (resolution to 0.1 pA) between parallel evaporated Al strips with 0.7 mm gap.

III. RESULTS AND DISCUSSION

A. General mechanism of disproportionation

FTIR can be effectively used to monitor the degree of oxygen content (x) in homogeneous SiO_x films, as the Si–O stretch frequency increases linearly from $\sim$965 to $\sim 1065\ cm^{-1}$ with oxygen content[12] as in Eq. (2). All reported stoichiometries for as-deposited films are calculated using Eq. (2) with observed ν_{Si-O}:

$$x = 0.020(\nu_{Si-O}) - 19.3. \tag{2}$$

Figure 1 shows the IR spectra and assigned vibrations for an as-deposited film and the effects of annealing treatments. The most important features due to annealing are the loss of Si–H modes, the increase in ν_{Si-O}, and increase in intensity of Si–O bend and rock modes. The gradual increase in ν_{Si-O} indicates that Eq. (3) describes the reaction chemistry, that is SiO_x disproportionates into a more oxygen rich suboxide $(x+y)$ and Si. The single Si–O stretch peak shape would be expected for either a homogeneous $SiO_{(x+y)}$ alloy or one with concentration gradients. Two distinct Si–O stretch peaks would form if only SiO_2+Si were formed, which is not observed:

$$SiO_x \rightarrow [x/(x+y)]SiO_{(x+y)} + [1 - x/(x+y)]Si, \tag{3}$$

$$\alpha = (\nu_m - \nu_i)/(\nu_f - \nu_i) \approx y/(2-x). \tag{4}$$

To quantify the kinetics of reaction (3), the extent of reaction (α) is given in Eq. (4), where reaction completion ($\alpha = 1$) is when $x+y=2$. ν_m is the measured ν_{Si-O}, ν_i is the as-deposited ν_{Si-O}, and ν_f is the measured ν_{Si-O} at completion (after anneals at 1000 °C with $\nu_{Si-O} \approx 1075\ cm^{-1}$). The integrated area of the Si–O stretch peak remains constant indicating no significant parasitic oxidation. With successive anneals the Si–O stretch peak becomes sharper and higher in frequency as expected in forming SiO_2.

Figure 2 shows the extent of reaction (α) of initial $SiO_{0.93}$ films as a function of time at various annealing temperatures. At all temperatures there is a rapid ($<$5 s resolution of RTA technique) initial reaction followed by a rate which is highly deceleratory. On this time scale, the reaction proceeds asymptotically to an extent of reaction less than completion. Si suboxide stability can be found through the kinetic hindrance of the disproportionation reaction. We propose a mechanism which is consistent with the observed kinetics. That is, an initial rapid segregation of SiO_x into a-Si which would by necessity form an SiO_2 shell. This shell acts as a diffusion barrier for continued reaction and explains the observed deceleratory behavior. The higher initial α with increasing anneal temperature is likely the result of a combination of increased nucleation density and increased growth rates.

To examine the temperature dependence of the kinetics, SiO_x films of various composition were annealed at successively higher temperatures. Each point of Fig. 3 is for an anneal of 6 min (where the reaction has decelerated appreciably) at the given temperature. For all compositions, the reaction is less hindered with increasing temperature. This suggests that higher temperatures allow for higher diffusion coefficients to negate the deceleratory diffusion barrier. The reaction kinetics are similar for all initial compositions. The notable exception is that the extent of initial reaction (anneal at lowest temperature, 600 °C) is greater for samples with lower oxygen content. This is consistent with an initial segregation into Si regions with the SiO_2 shell. By a simple stoichiometric argument, less oxygen content will by necessity require more SiO_x to decompose to form an SiO_2 shell at a given nucleation density. Figure 4 shows a cross-sectional transmission electron microscope (TEM) micrograph of $SiO_{1.0}$ after an anneal at 900 °C. Si nanocrystals are formed

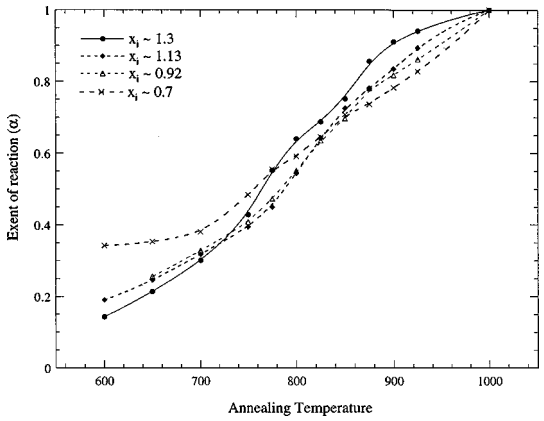

FIG. 3. Extent of reaction (α) for SiO_x (initial $0.7<x_i<1.3$) thin films as a function of annealing temperature showing nearly linear progression of α. Each composition is annealed sequentially on the same film with annealing times of 6 min for each temperature.

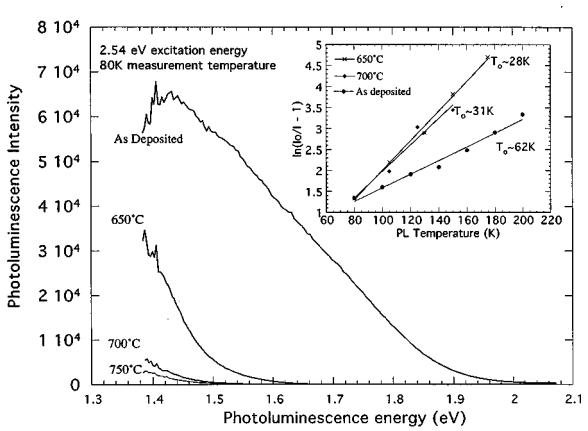

FIG. 5. Photoluminescence of $SiO_{0.93}$ after sequential annealing at various temperatures for 6 min, followed by low temperature H_2 plasma treatment. No PL is observed in annealed samples without H_2 plasma treatment. Inset shows $\ln(I_0/I-1)$ vs T. Annealed samples (1/slope) give T_0 of 28–31 K which is near the characteristic of T_0 of a-Si (25 K).

in an amorphous SiO_2 matrix, consistent with a mechanism of Si segregation with the SiO_2 shell. TEM micrographs of films annealed at 750 °C are completely amorphous; thus the disproportionation reaction proceeds in the amorphous state, not requiring a crystalline growth interface.

SiO_x and amorphous silicon (a-Si) have well known PL properties and can be readily applied to this system to demonstrate the phase segregation in the amorphous state. Figure 5 shows the characteristic visible PL of as-deposited $SiO_{1.3}$. With modest annealing $>\sim$500 °C all PL is lost, due to nonradiative carrier recombination with Si dangling bond defects. Only after treatment of annealed films in H_2 plasma, to passivate Si dangling bonds, is PL restored, similar to results with a-Si after moderate anneals.[13] This PL coincides with the characteristic energy of a-Si (1.3 eV). The inset of Fig. 5 shows the dependence of PL on measurement temperature. The treatment of $\ln(I_0/I-1)$ vs T is commonly applied to amorphous Si with the slope being a characteristic temperature (T_0) for carriers to hop from localized states in band tails to conduction band.[14] With higher T_0, PL is more stable to increasing measurement temperature. As-deposited $SiO_{1.3}$ has a T_0 near 63 K while after annealing the temperature stability is markedly reduced to T_0 of 29 K, which is nearly identical to a-Si ($T_0\sim$25 K). Optical absorption measured band gap is also consistent with the segregation forming a-Si, with the $E04$ decreasing from 2.2 to 1.8 eV after annealing (1.8 eV is characteristic of a-Si).

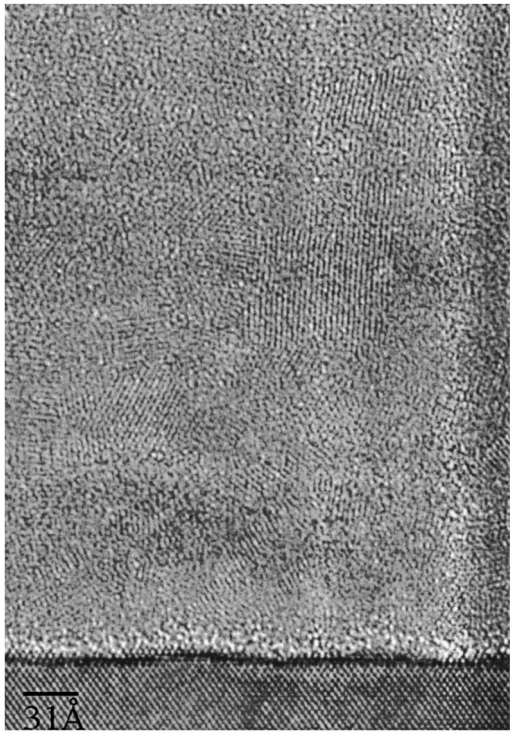

FIG. 4. Cross-sectional TEM of initial $SiO_{1.0}$ after annealing at 900 °C for 30 s clearly showing $SiO_x \rightarrow Si_{nc}+SiO_2$. At lower temperatures $<\sim$800 °C films are completely amorphous.

Observations in conductivity measurements also support an amorphous state segregation mechanism. Figure 6 shows both the dark- and photocurrent of films of various composition before and after annealing at 650 °C. For as-deposited films, the dark current is very low indicating a low level of Si dangling bond density. With increasing O content, the photocurrent decreases, which is expected for decreased absorption coefficient. After annealing, the dark current increases markedly as expected from the formation of Si dangling bonds. However at high O content, the photocurrent after annealing actually increases because of the increase in absorbance from a-Si regions. Both dark current and photocurrent decrease exponentially with increasing O content, which is consistent with a segregation model in which conduction paths between a-Si regions is reduced. Both PL and conductivity measurements show that Si dangling bond defect density is significant. Therefore it is of importance to determine whether the kinetics of SiO_x disproportionation are accelerated by defects. Figure 7 shows the extent of reaction as a function of annealing temperature for films of different initial H content. A factor of two difference in initial Si–H

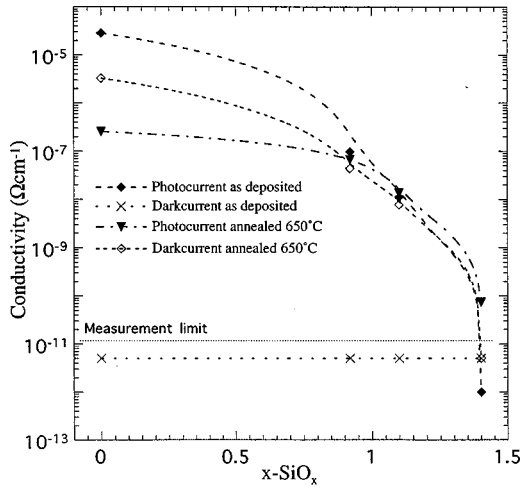

FIG. 6. Dark and photoconductivity measurements of various SiO_x films before and after anneals at 650 °C for 6 min. Changes in conductivity are consistent with a phase segregation in the amorphous state.

concentration does not effect observed kinetics, thus is not likely to be involved in the dominate mechanism.

B. Kinetic modeling

The previous experimental observations support the general mechanism of an initial rapid segregation of SiO_x into a-Si with an SiO_2 diffusion barrier which decelerates further reaction. This mechanism would also form a concentration gradient resulting in an oxygen rich $SiO_{(x+y)}$ matrix. To model the kinetics, we can apply the three-dimensional (3D) Avrami–Erofe've approach [Eqs. (5)–(7)] in which there is an instantaneous nucleation followed by a diffusion limited growth process.[15] α is the extent of reaction, N_c is nucleation density (cm^{-3}), D is diffusion coefficient (cm^2/s), and t is time of reaction in seconds. In this treatment an alloy of matrix composition (C_m, SiO_x) decomposes into nucleation sites of β phase (C_β, a-Si) and α phase (C_α, SiO_2) which acts as a diffusion barrier for the growth of β phase. This geometry is schematically shown in the inset of Fig. 8. With

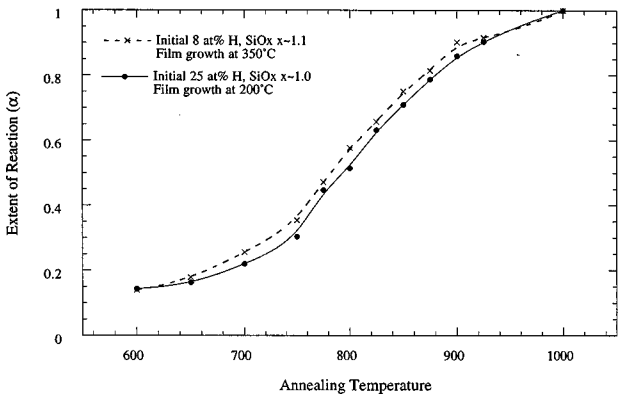

FIG. 7. Extent of reaction (α) for SiO_x thin films with different initial H content, as a function of annealing temperature showing nearly identical kinetics. Each series is annealed sequentially on the same film with annealing times of 6 min for each temperature.

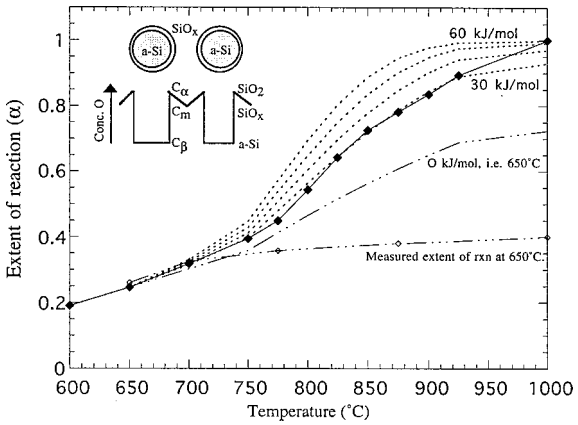

FIG. 8. Application of Avrami–Erofe've 3D treatment [Eqs. (5)–(7)] to observed α of $SiO_{1.1}$ decomposition (solid line). Inset figure shows geometry of transformation and oxygen gradient involved. Each solid point is a successive anneal at given temperature for 6 min. The dashed lines are calculated using activation energy (E_a) shown (30–60 kJ/mol). The open diamond points are isothermal data at 650 °C with times corresponding to cumulative times of temperature ramped data, which do not agree with predicted α ($E_a=0$ kJ).

O as the diffusion species, $C_x=(2.27\times10^{22}\ cm^{-3})\cdot x$, $C_\alpha=4.55\times10^{22}\ cm^{-3}$, $C_\beta=0$, R_f is the final Si_{nc} radius, and V_f is the final Si volume fraction calculated from stoichiometry (x). N_c is $1\times10^{18}/cm^3$ (from TEM size measurements at $\alpha=1$):

$$\ln(1-\alpha)=\frac{8\sqrt{2}\pi}{3}N_0D^{3/2}\left(\frac{(C_m-C_\alpha)}{(C_\beta-C_\alpha)}\right)^{1/2}t^{3/2}, \tag{5}$$

$$D=D_0\ \exp(-E_a/kT), \tag{6}$$

$$N_c=\frac{4/3\pi R_f^3}{V_f},\quad V_f=\frac{1-x/2}{1+0.6x}. \tag{7}$$

In Fig. 8, the solid points are the extent of reaction for initial $SiO_{1.1}$ after successive annealing for 6 min at each temperature. The dashed lines are calculated from Eqs. (5)–(7) using the activation energy (E_a) shown and the initial reaction rate at 650 °C. In other words, the rate of reaction at 650 °C (i.e., $\Delta\alpha$ 600–650 °C) is used to calculate D_0 for a given E_a. This D_0 and E_a are used to calculate α at successively higher temperatures for the 6 min periods, resulting in the dashed line in Fig. 8. As can be seen in Fig. 8, rather low activation energies of 30 kcal/mol are found to fit experimental data. This treatment predicts significant reaction at 650 °C while isothermal experiments (Fig. 2) show significant deceleration well before reaction completion. This is best seen in Fig. 8, where the calculated extent of reaction at 650 °C ($E_a=0$) is compared to experimental data (open diamonds) for anneals at 650 °C (in this case the x axis acts as time instead of temperature). The measured kinetics are significantly decelerated compared to those predicted. There is a fundamental inadequacy of the 3D Avrami–Erofe've treatment. That is while diffusion barrier decelerates the reaction by a factor of $\sqrt{2}$, the volume of a-Si phase grows as the cube of radius. This results in an overall $t^{3/2}$ dependence, which is accelerator. Significant deceleration would occur only near comple-

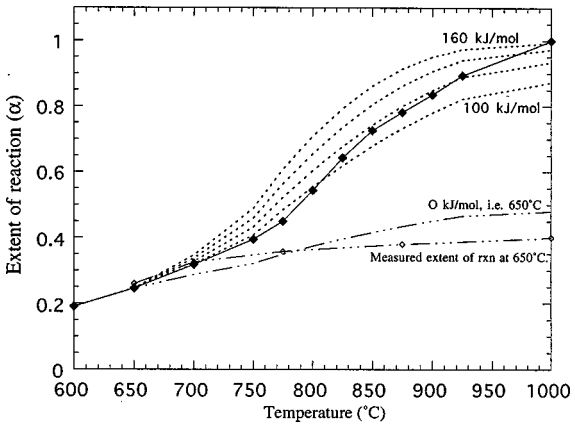

FIG. 9. Application of Avrami–Erofe've 1D treatment [Eqs. (8)–(9)] to observed α of $SiO_{1.1}$ decomposition (solid line). Each solid point is a successive anneal at given temperature for 6 min. The dashed lines calculated using shown activation energy (E_a) (100–160 kJ/mol). The open diamonds are isothermal data at 650 °C with times corresponding to cumulative times of temperature ramped data, which approach predicted α ($E_a=0$ kJ).

tion ($\alpha>0.8$) from impingement, which is not experimentally observed. Thus the 3D Avrami–Erofe've treatment is not directly applicable to this system.

To account for the highly deceleratory nature of the reaction we can look at the dimensionality of phase growth. Typically the dimensionality of a reaction is found by microstructure of the resultant products, i.e., spherical particles imply 3D growth, platelets 2D, and needles 1D. The observed spherical Si nanocrystals imply 3D growth, however this may not necessarily reflect reactions in the amorphous state. The Si nanocrystals may be nucleated and grown in existing *a*-Si regions, representing a different reaction, which is 3D. Crystallization of *a*-Si regions in SIPOS has been similarly proposed from Raman experiments.[16] Since the initial segregation in amorphous Si is extensive, it is possible to have volume growth without significantly expanding surface area. Impingement upon itself and regions of decreasing reaction surface area will reduce the dimensionality of the growth reaction. Equation (8) describes the Avrami–Erofe've for the 1D limit:

$$\ln(1-\alpha)=\frac{A_i(C_m-C_\alpha)}{(C_\beta-C_\alpha)^{1/2}(C_\beta-C_m)^{1/2}}\,D^{1/2}t^{1/2}, \tag{8}$$

$$A_i=\frac{V_f}{d_f}, \tag{9}$$

where A_i is the initial surface area of the amorphous Si region after initial segregation reaction which is approximated by Eq. (9) and d_f is the average Si nanocrystal diameter as seen by TEM. Figure 9 shows the fit of Eq. (8) using the same method used in Fig. 8. The reduced dimensionality increases activation energy to 120 kJ/mol. Table I shows calculated parameters for 1D Avrami–Erofe've treatment. The extent of reaction (α) calculated for 650 °C ($E_a=0$) approaches that observed isothermal data shown in Fig. 9. Thus 1D Avrami–Erofe've is a reasonable limit for the observed kinetics. If we apply the calculated *D* to the initial

TABLE I. Parameters for kinetic data of $SiO_{1.1}$ disproportionation shown in Fig. 9 which are fit to 1D Avrami–Erofe've treatment [Eqs. (8)–(9)].

$x_i=1.1$	End thickness=50 Å
$E_a=120$ kJ/mol	$D_0=5.5\times10^{-9}$ cm^2/s
$D(650\ °C)=8.9\times10^{-16}$ cm^2/s	
$D(900\ °C)=2.4\times10^{-14}$ cm^2/s	
Linear growth rate ($\alpha_i=0.19$, 650 °C)=0.04 Å/s	
Linear growth rate ($\alpha_i=0.09$, 900 °C)=1.2 Å/s	

barrier ($\alpha=0.19$) we find a rapid linear growth rate near 1.2 Å/s at 900 °C. This rate is significantly faster and with lower E_a than the observed by Nesbit's treatment of Si_{nc} growth ($E_a\sim180$ kJ/mol), suggesting that those kinetic values are for the crystallization of *a*-Si with O impurities. This interpretation is further supported by recent work which has shown that as-deposited SIPOS films have significant segregation into *a*-Si regions (~50%).[17]

C. Uncertainty in kinetic parameters

It is important to quantify the uncertainties in the kinetic parameters found in the 1D Avrami–Erofe've treatment. Most significant is the uncertainty of IR measurements. As-deposited films contain significant amounts of Si–H which broaden the Si–O stretch peak and adds uncertainty to ν_i in Eq. (4). Uncertainty in ν_i will shift the position of all measured α. The most extreme case is if the observed shift in ν_{Si-O} after the 600 °C anneal was due solely to H loss and not to the reaction in Eq. (4). Using the kinetic treatment as in Fig. 9 on this limiting case would result in an E_a of 170 kJ/mol. However photoluminescence, ultraviolet visible (UV-vis) absorption, conductivity, and Raman data all show the presence of *a*-Si after low temperature anneals, thus there must be a disproportionation reaction at these low temperatures with simultaneous H loss. The data in Fig. 7 also strongly suggest the H content does significantly shift the Si–O stretch position. A factor of two reduction in the initial H content did not change α observed at 600 °C. A 50% error in α after 600 °C anneal would result in an E_a of 135 kJ/mol. Viscoelastic relaxation can play a role in shifting ν_f. Using α at 925 °C as *a* the lower limit where viscoelastic effects are known to be minimal, the maximum error in the derived E_a is +5 kJ/mol. Thus the E_a value of 120 kJ/mol for the 1D Avrami–Erofe've treatment is a lower limit with an uncertainty of +20 kJ/mol.

Any significant nucleation rate after initial rapid segregation would result in an accelatory reaction rate, which is not observed. A possibility is that there is no growth of existing nuclei and the measured extent of reaction is only due to forming new nuclei. The observed deceleration could be explained as function of a reduction in nucleation rate. An increase in temperature may allow otherwise hindered sites to nucleate. It is difficult to separate this effect from the growth of existing nucleation centers as in the Avrami–Erofe've treatment. This effect can be discounted for several reasons. Generally, impingement effects which decelerate nucleation typically are seen at $\alpha\sim0.8$. Yet this system of deceleration

occurs around $\alpha \sim 0.2-0.4$. If only a nucleation mechanism were present, an SiO_2 shell would be formed and the IR measurements would show two peaks corresponding to SiO_2 and SiO_x, not the observed gradient. Thus there must be an a-Si phase growth mechanism. Any effects of nucleation at higher temperature would increase observed transformation rates, thus the E_a derived from the 1D Avrami–Erofe'ye treatment is a lower limit.

IV. CONCLUSIONS

SiO_x metastability in thick films can be found through kinetic hindrance. The disproportionation reaction proceeds by (1) rapid (<5 s) initial segregation forming a-Si and SiO_2 diffusion barrier, (2) highly deceleratory growth of a-Si regions form $SiO(x+y)$ diffusion gradient, (3) crystallization of a-Si regions into Si nanocrystals. FTIR, PL, TEM, Raman, and conductivity measurements all support a model with significant disproportionation in the amorphous state. Analysis of the highly deceleratory kinetics shows that the initial a-Si regions is extensive and growth is of low dimensionality. The 1D limit of Avrami–Erofe'ye treatment gives lateral growth rates of 1.2 Å/s (900 °C) and 0.04 Å/s (650 °C) with an activation energy of 120 kJ/mol, after initial segregation reaction. Due to the rapid initial segregation and relatively large lateral growth rate, a simple kinetic hindrance explanation for the 4–8 Å of interfacial SiO_x at the SiO_2/Si interface is unlikely.

ACKNOWLEDGMENTS

The authors would like to thank Meimei Xu and Professor Denis Maher for the collection of TEM data. This research has been funded by the National Science Foundation and Office of Naval Research.

[1]F. J. Grunthaner and P. J. Grunthaner, Mater. Sci. Rep. **1**, 65 (1986).
[2]T. Hatttori and T. Suzuki, Appl. Phys. Lett. **43**, 470 (1983).
[3]L. Brewer and R. K. Edwards, J. Electrochem. Soc. **58**, 351 (1954).
[4]M. Hamasaki, T. Adachi, S. Wakayama, and M. Kikuchí, J. Appl. Phys. **49**, 3987 (1978).
[5]J. Liday, S. Tomek, and J. Breza, Appl. Surf. Sci. **99**, 9 (1996).
[6]B. Greenberg and T. Marshall, J. Electrochem. Soc. **135**, 2295 (1979).
[7]G. Kragler, H. Bender, G. Willeke, E. Bucher, and J. Vanhellemont, Appl. Phys. A: Solids Surf. **58**, 77 (1994).
[8]M. Catalano, M. J. Kim, R. W. Carpenter, K. Das Chowdhury, and J. Wong, J. Mater. Res. **8**, 2893 (1993).
[9]D. J. Nesbit, Appl. Phys. Lett. **46**, 38 (1986).
[10]A. Banerjee and G. Lucovsky, in *Amorphous Silicon Technology-1996*, edited by M. Hack, R. Schropp, E. A. Schiff, A. Matsuda, and S. Wagner, Mater. Res. Soc. Proc. (MRS, Pittsburgh, PA, in press), Vol. 420.
[11]G. Lucovsky, D. V. Tsu, R. A. Rudder, and R. J. Markunas, in *Thin Film Processes II*, edited by J. L. Vossen and W. Kern (Academic, San Diego, CA, 1991), pp. 565–619.
[12]D. V. Tsu, G. Lucovsky, and B. N. Davidson, Phys. Rev. B **40**, 1795 (1989).
[13]J. I. Pankove, Appl. Phys. Lett. **32**, 812 (1978).
[14]R. A. Street, Adv. Phys. **30**, 593 (1981).
[15]M. E. Brown, D. Dollimore, and A. K. Galwey, in *Comprehensive Chemical Kinetics, Volume 22 Reactions in the Solid State*, edited by C. H. Bamford and C. F. H. Tipper (Elsevier, Oxford, 1980), pp. 68–78.
[16]D. J. Olego and H. Baumgart, J. Appl. Phys. **63**, 2669 (1988).
[17]M. Trchova, J. Zemek, and K. Jurek, J. Appl. Phys. **82**, 3519 (1997).